Sigma J Eng Nat Sci, Vol. 39, No. 4, pp. 374-391, December, 2021

Sigma Journal of Engineering and Natural Sciences
Web page info: https://sigma.yildiz.edu.tr
DOI: 10.14744/sigma.2021.00026

Research Article

Estimation of ground types in different districts of Gümüşhane province based on the ambient vibrations H/V measurements

Serkan ÖZTÜRK[1,*], Yasemin BEKER[2], Mahmut SARI[3], Levent PEHLİVAN[4]

[1]*Department of Geophysics, Faculty of Engineering and Natural Sciences, Gümüşhane University, Gümüşhane, Turkey*
[2]*Department of Geophysics, Faculty of Engineering and Natural Sciences, Gümüşhane University, Gümüşhane, Turkey*
[3]*Gümüşhane Vocational School, Gümüşhane University, Gümüşhane, Turkey*
[4]*Department of Geophysics, Faculty of Engineering and Natural Sciences, Gümüşhane University, Gümüşhane, Turkey*

ARTICLE INFO

Article history
Received: 19 October 2020
Accepted: 14 January 2021

Key words:
Gümüşhane; Microtremor; Predominant frequency; H/V ratio; Kg-value; Ground type

ABSTRACT

In this study, an attempt was made to estimate the ground types for Torul, Kürtün, Kelkit, Şiran and Köse districts of Gümüşhane, Turkey, by analyzing the predominant frequency and H/V ratio from microtremor data through the single station microtremor H/V ratio of Nakamura technique. For all districts, predominant frequencies show a general distribution between 1.36 and 9.84 Hz, H/V ratios between 1.01 and 9.58. According to these variations, three transient zones can be suggested as *i*) Z_1, stiff rock composed of gravel, sand and other soils mainly consisting of tertiary or older layers with period of 0.1 to 0.2s, *ii*) Z_2, sandy gravel, stiff sandy clay, loam or sandy alluvial deposits whose depths are 5m or greater with period of 0.2 to 0.4s, and *iii*) Z_3, standard grounds other than type Z_1, Z_2 or Z_4 (alluvial deposits whose depths are 5m or greater) with period of 0.4 to 0.8s. These results suggest that predominant period obtained from predominant frequency shows significant changes based on the soil formation, and H/V ratio highly corresponds to these subsurface properties. Soil-structure interaction can also be evaluated by considering these results and possible resonance risk can be investigated for building resonant frequency in these residential districts in the next. Thus, this type of application and evaluation of microtremor data may provide primary and useful information for other geophysical, geological and geotechnical studies such as planning the seismic resistant infrastructure, detecting the small-scale seismic risks and making a suitable and reliable seismic hazard microzonation in Gümüşhane.

Cite this article as: Öztürk S, Beker Y, Sari M, Pehliva L. Estimation of ground types in different districts of gümüşhane province based on the ambient vibrations H/V measurements. Sigma J Eng Nat Sci 2021;39(4):000–000.

***Corresponding author.**
*E-mail address: serkanozturk@gumushane.edu.tr

This paper was recommended for publication in revised form by Regional Editor Barış Sevim

INTRODUCTION

There are various techniques that have been used in order to identify the subsoil characteristics during the strong ground motions. One of the most widely applied techniques to estimate the ground types is the microtremor horizontal to vertical (H/V) ratio. This technique was defined by Nakamura [1] in relation to borehole explorations and analysis of strong ground motion data on the different geological structures. Many researchers have used the spectral features of microtremors to estimate the predominant or natural frequency of the soil in Turkey and different sites of the world. These studies suggest a good relationship between the surface geology and the spectral ratios of microtremors [1–11]. These results show that microtremors are very suitable tools in the identification of surface geological effects on the seismic motion without detailed geology.

Microtremors are always exist and known as weak ground motions based on the natural or ambient processes such as earthquakes, sea waves, wind, rivers, rain, traffic, tides, changes in atmospheric pressure, human activities, machinery, etc. Their amplitudes vary from 0.1 to 1.0 μm, periods between 0.05 and 2.0s, and these motions change the site effects [11–13]. Observations and assessments of microtremor data have some advantages over other techniques for site response characteristics due to its simplicity, inexpensive, ease of use, minimum computational time, short duration for measurements and data process [2,6]. General applications of microtremor studies can be carried out: (*i*) to calculate the amplification of horizontal movements in the free surface throughout earthquakes, (*ii*) to measure background seismic noise and to estimate the mechanical features of the earth's subsurface, (*iii*) to determine the site response characteristics, (*iv*) to detect the subsoil types, (*v*) to estimate the shear wave velocity of the ground, (*vi*) to detect the effect of site conditions on damage distribution during the earthquakes, (*vii*) to estimate the predominant resonant frequency and period of the sediments, (*viii*) to design the seismic resistant infrastructure, (*ix*) to identify small-scale seismic risks and to make a convenient and reliable seismic hazard microzonation in urban areas [14–17].

The H/V spectral ratio of recorded microtremors can be estimated from ambient noise records and this technique is quite practical tool for engineers to measure the intensity of earthquake ground motion and the capacity of buildings to resist earthquakes [6]. For this purpose, we used the single station microtremor H/V spectral ratio technique in this study and aimed to investigate the seismic site response characteristics in Torul, Kürtün, Kelkit, Şiran and Köse districts of Gümüşhane province, Turkey. For this purpose, we determined the predominant frequency and H/V ratio (H/V amplitude spectrum or HVSR amplitude) of subsurface ground using measured microtremor data. Thus, a classification for ground types in different districts of Gümüşhane was made based on the single station microtremor data analysis.

SURFACE GEOLOGY AND SEISMOTECTONICS OF GÜMÜŞHANE

The Gümüşhane is located in the eastern part of the Pontide Orogenic belt in the northeast Turkey. The principal base rocks observed in Gümüşhane and vicinity are composed of the Palaeozoic-aged metamorphic rocks and Gümüşhane granites which rise by cutting these metamorphic rocks (One can find many details on geological ages in Taş et al., [18]). Surface geology in and around Gümüşhane is modified from the database of the General Directorate of Mineral Research and Exploration (MTA, URL-1) and given in Figure 1. Granitic formations are dominated in Gümüşhane city center and the main geological units close to the city center are formed of granite, granodiorite and quartz-diorite, Eosene-volcanic facies, undifferentiated Cretaceous, upper Cretaceous and Flysch. Torul district and surrounding area are generally covered with granite, granodiorite, quartz-diorite and Eosene-volcanic facies. The principal surface geology in Kürtün district and vicinity includes granite, granodiorite, quartz-diorite and upper Cretaceous-Volcanic facies. Geological formations of undifferentiated Eocene, Eocene flysch, mid-Eocene lutetian, andesite-spilite-porphyrite, basalt-dolerite, rhyolite-dacite and volcanic tuff-agglomerate-breccia are dominant in and around Şiran district. However, Kelkit and Köse districts are composed of the Pleistocene and Holocene-Recent structures, undifferentiated Neogene continental formations, undifferentiated Eocene, Eocene flysch, mid-Eocene lutetian floors and partially granite, granodiorite, quartz-diorite structures.

The major factors that affect the current seismotectonic situation of Gümüşhane and vicinity are fracture systems and fold tectonics. Tectonic structures of Gümüşhane and vicinity were compiled from Şaroğlu et al. [19] and Bozkurt [20] and were shown in Figure 2. There are several fault segments, zones and basins located close to Köse, Kelkit, Şiran, Erzincan and Bayburt, and these tectonic structures are generally related to the NAFZ. As seen in Figure 2, these active systems can be given as Kelkit-Çoruh Fault Zone (KÇFZ), Bayburt Basin (BYB), Kelkit Basin (KLB), Kelkit Fault Segment (KLFS), Akdağ-Çayırlı Fault Zone (AÇFZ), Dağyolu Fault (DYF) and Tercan-Aşkale Fault Zone (TAFZ). KÇFZ is about 600 km long and has a left lateral strike slip fault mechanism. This zone has four segments from the southwest to the northeast: Kelkit, Çoruh, Posof and Borjomi-Kasbeg. KLFS is separated from the NAFZ with a length of about 100 km. This segment is divided into two branches around Kelkit and results in a basin [18]. TAFZ has a left lateral strike slip fault mechanism. It has a length of about 150 km and a wide of 2 to 4 km. This fault zone passes through the western part of Erzurum near the

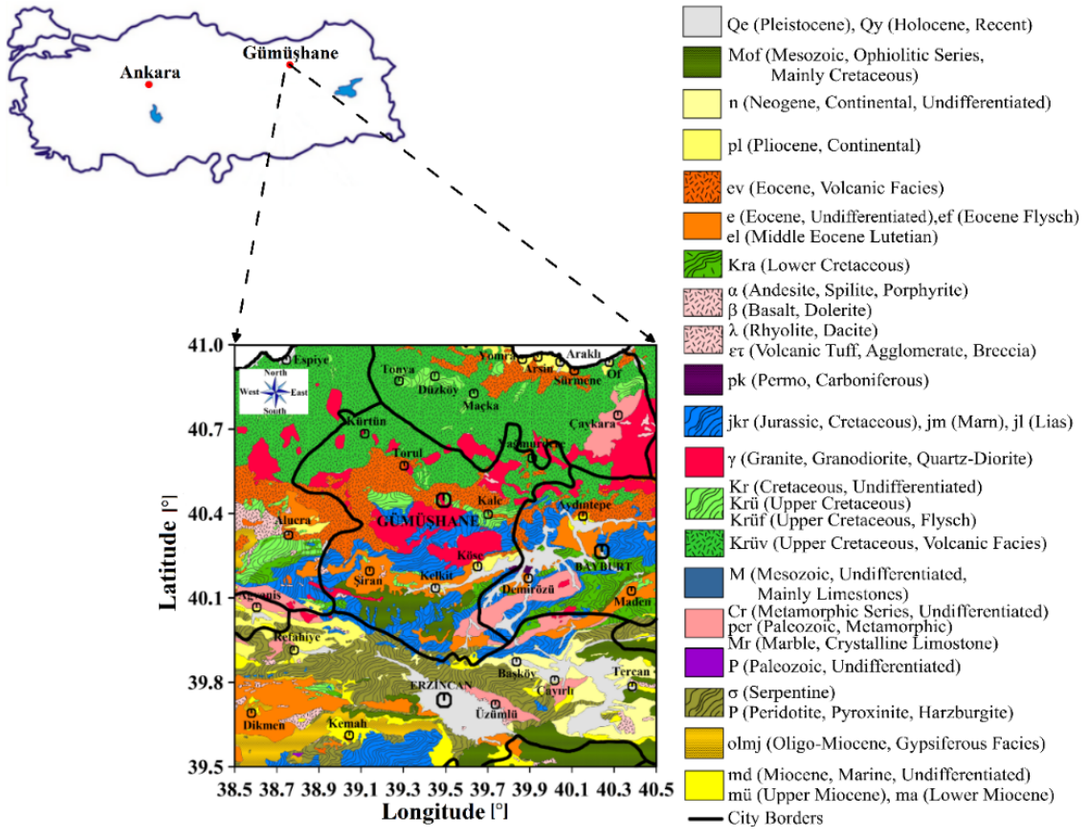

Figure 1. Detailed near surface geology and different formations in and around Gümüşhane province (digitized from MTA, URL-1).

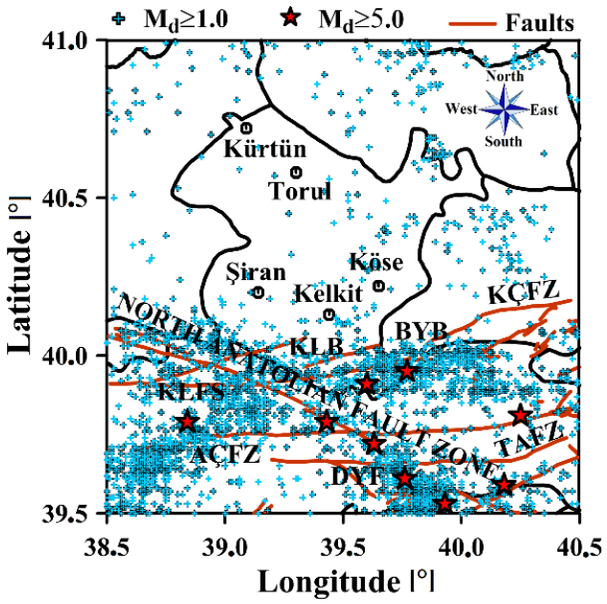

Figure 2. Seismic and tectonic structures in Gümüşhane and surroundings between 1970 and mid-2018. Simplified tectonics were modified from different sources such as Şaroğlu et al., [19] and Bozkurt [20].

NAFZ and includes several parallel fault segments which has a length between 2 and 20 km [20].

Gümüşhane is a very close residential area to the North Anatolian Fault Zone (NAFZ), about 80 km, and due to the proximity to the NAFZ, a strong or large earthquake on the NAFZ and surrounding area may affect this region. Especially, high-rise buildings constructed on alluvial grounds in creek beds along the Harşit stream will be affected from a possible large and/or destructive earthquakes which may occur on the NAFZ [21]. During the instrumental (past 48 years in this study) and historical periods, there are two strong events around Gümüşhane border as seen in Figure 2: January 19, 1979 (M_d5.0) and August 12, 1985 (M_d5.0) earthquakes (M_d is duration magnitude). Also, several large and destructive earthquakes occurred in and around the NAFZ between 1970 and mid-2018 such as March 13, 1992 (M_d6.5) and March 15, 1992 (M_d5.3), whereas the other great events occurred in some parts of Gümüşhane near the NAFZ. Figure 2 shows the epicenter distributions of earthquakes (depth ≤ 75 km) with $1.0 \leq M_d \leq 6.5$ from 1970 to middle of 2018.

METHODOLOGIES AND MICROTREMOR DATA FOR STUDY REGIONS

The H/V Spectral Ratio Method

Microtremor H/V spectral ratio technique was developed by Nakamura [1] on the different geological ground circumstances related to the borehole surveys by using the analyses of strong ground motion. Nakamura [1] supposed that vertical component of the ambient noise at the ground surface includes the properties of basement ground. Therefore, Rayleigh waves on the sedimentary rock influence the vertical component and thus, vertical component can be utilized to eliminate both of the source and Rayleigh wave effects from horizontal components [22]. In fact, the first of all, the H/V spectral ratio was provided with the strong motion measurements at different parts of Japan. Then, many researchers mentioned above showed that microtremor H/V spectral ratio of ambient noise may be utilized to describe the predominant frequency and H/V ratio of different ground structures in different regions of the world. Nakamura [1] assumes that microtremors mainly contain the shear waves, and the layer of soft soil does not magnify the vertical waves. The horizontal components of the shear waves are magnified by soft soil layer because of the multiple reflection of the waves [13]. There are four amplitude spectra described in the Fourier frequency domain. Nakamura [1] suggested that the H/V spectral ratio of the Fourier amplitude spectra of microtremors can be used to estimate the transfer function of the surface layers. Microtremor movements were described as a function of frequency:

$$A_S(\omega) = \frac{V_S(\omega)}{V_B(\omega)} \tag{1}$$

$$S_E(\omega) = \frac{H_S(\omega)}{H_B(\omega)} \tag{2}$$

where $V_S(\omega)$ is the vertical component of the movement on the surface and $V_B(\omega)$ is the vertical component of the movement on the substrate of the surface layer. Equation (2) represents the transfer function in measurement point. In this equation, $H_S(\omega)$ is the horizontal component on the surface and $H_B(\omega)$ is the horizontal component of the movement on the substrate of the surface layer. Source effect can be removed from observation values by dividing transfer function given in Equation (2) to source effect given in Equation (1). This rate is defined as:

$$\begin{aligned} S_M(\omega) &= \frac{S_E(\omega)}{A_S(\omega)} = \frac{\frac{H_S(\omega)}{H_B(\omega)}}{\frac{V_S(\omega)}{V_B(\omega)}} = \frac{H_S(\omega)}{H_B(\omega)} \cdot \frac{V_B(\omega)}{V_S(\omega)} \\ &= \frac{H_S(\omega)}{V_S(\omega)} \cdot \frac{V_B(\omega)}{H_B(\omega)} = R_S(\omega) \times R_B(\omega) \end{aligned} \tag{3}$$

Nakamura [1] stated that the H/V spectral ratio, $R_B(\omega)$, taken in bedrock in the frequency range of interest (1–20 Hz) for engineering purposes studies, is approximately equal to 1 as given in Equation (4). In this way, the transfer function described as $R_S(\omega)$ can be obtained from microtremor data measured at the surface:

$$R_B(\omega) = \frac{V_B(\omega)}{H_B(\omega)} = 1 \tag{4}$$

Two horizontal components recorded as north-south, NS (ω), and east-west, EW (ω), can be combined as a single component taking the magnitude of the vector as described in Equation (5):

$$H_S(\omega) = \sqrt{NS(\omega)^2 + EW(\omega)^2} \tag{5}$$

The ground effect is described in terms of the horizontal and vertical components at the surface. The H/V spectral ratio can be obtained by dividing horizontal component, $H_S(\omega)$, to vertical component, $V_S(\omega)$, as described in Equation (6):

$$S_M(\omega) = \frac{H_S(\omega)}{V_S(\omega)} \tag{6}$$

Evaluation of the H/V ratio was achieved by using the GEOPSY software developed within the framework of the Site Effects Assessment using Ambient Excitation (SESAME) Project [23]. The first step involved in applying the H/V spectral ratio technique, recorded signals were fixed with a baseline correction and trend effects in the data were removed. Then, corrected records were filtered with a Butterworth band pass filter with a range of 0.5–20 Hz. In the third stage, several window lengths in the range of 10–40s were tested to find the suitable window size and a 20s time window length was preferred. For each window, a Cosine taper filter with 10% width was implemented to decrease border effects caused by the cutting operation. In this way, the noise at very low and high frequencies compared to the signals was removed, and only the frequency content of the microtremors remain. In the next step, the fast Fourier transform (FFT) was utilized to calculate the three component (north-south, east-west and vertical) amplitude spectrum. For each window, the signal in the time domain was converted to frequency domain. In order to smooth the computed spectrum, a smoothing type filter defined by Konno and Ohmachi [24] was used with constant number of 40. In this way, the small noises from the resulting spectrum were removed and a good approximation with clear spectrum peaks was generated by this smoothing coefficient. In the next stage, the root mean square of spectrum values for two horizontal components (north-south and east-west) was taken and the single horizontal component

was obtained. Thus, horizontal component direction was computed independently and the noise ratio on any of components was reduced. In the final step, the average of horizontal components (root mean square) was divided by the vertical component spectrum for all windows, and an average spectrum was computed with its confidence intervals to estimate the resonant frequency with respect to high amplitude peak. The H/V spectral ratio for suitable windows was obtained and then, the average of the spectra was accepted as the H/V spectral ratio for each measurement point. Representative H/V spectral ratio curves were plotted for each measurement point according to the standard criteria of SESAME [23]. As a result, the peak frequency of the H/V spectrum plot gives the dominant frequency and H/V ratio of the measured point. Figure 3 shows all these data processing steps with an example measurement point from Köse district.

Study regions and measurement points for Torul, Kürtün, Kelkit, Şiran and Köse districts of Gümüşhane province were shown in Figure 4. Measurement points were placed on "Google Earth" in order to obtain the best images of the point and to see the settlements in each individual site. A total of 180 single station microtremor measurements were conducted to estimate the predominant frequency and H/V ratio. For this purpose, GURALP CMG-6TD three component broad band velocity seismometer was used. Measurements were recorded numerically in GCF (Guralp Compressed Format) with Scream 4.5 program. The locations of the recording points and the distance between the them were chosen as close to the settlement areas, taking into account the size and layout of the survey area. Distances between microtremor measurement points range from 100 to 500 m depending on the density of the settlement area. The recording time was determined by considering the content of the noise and generally varies from 10 to 30 minutes. Thus, the transfer function (H/V spectral ratio) of surface layer as described by Equation (6) was estimated only from the tremor on the surface. This ratio between vertical and horizontal components of the measured at the surface is defined the site effects as $S_M(\omega)$. This mean that H/V ratio can be used a reliable application of the site response to shear wave, supplying reliable results, not only for the resonance frequency, but also for the corresponding amplification [7].

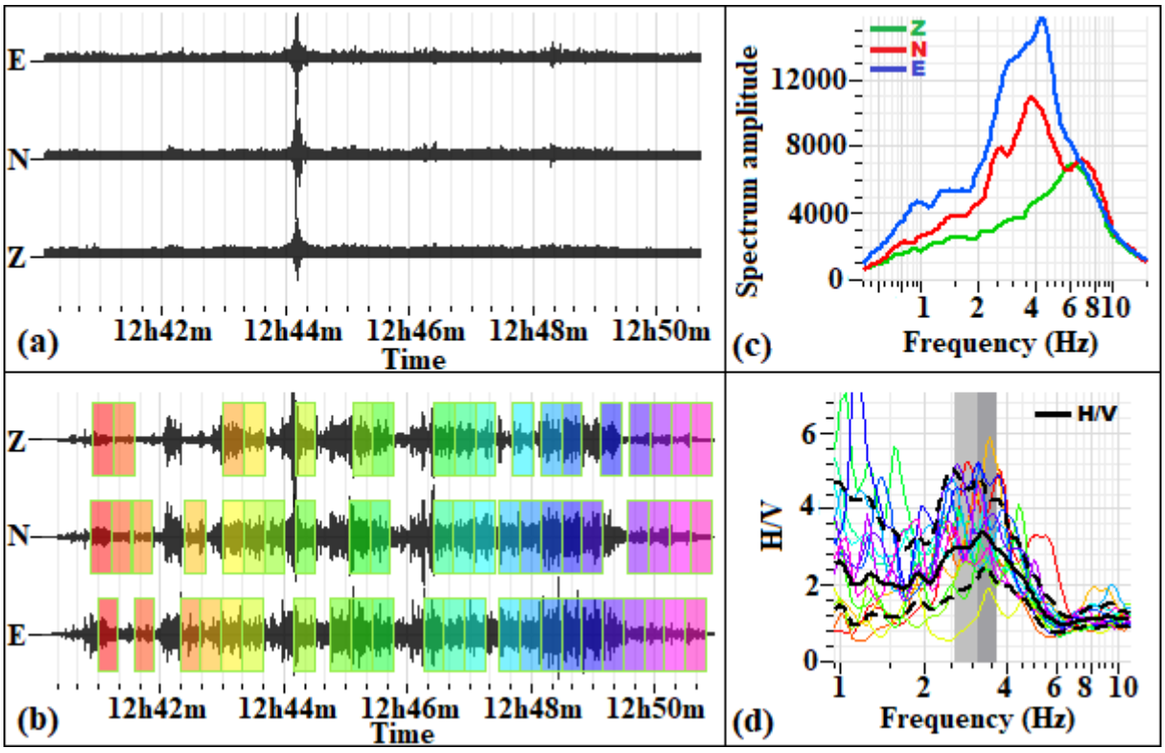

Figure 3. Data processing steps for the H/V spectral ratio calculations. These processes were applied all measurement points in study region. This example includes KS38 point: (a) raw microtremor data, (b) analysis window (number of windows: 63, length=20s), (c) average spectrums of three components and (d) H/V spectral ratio of each window (color lines), mean H/V ratio spectrum (black line) and standard deviation (dashed line).

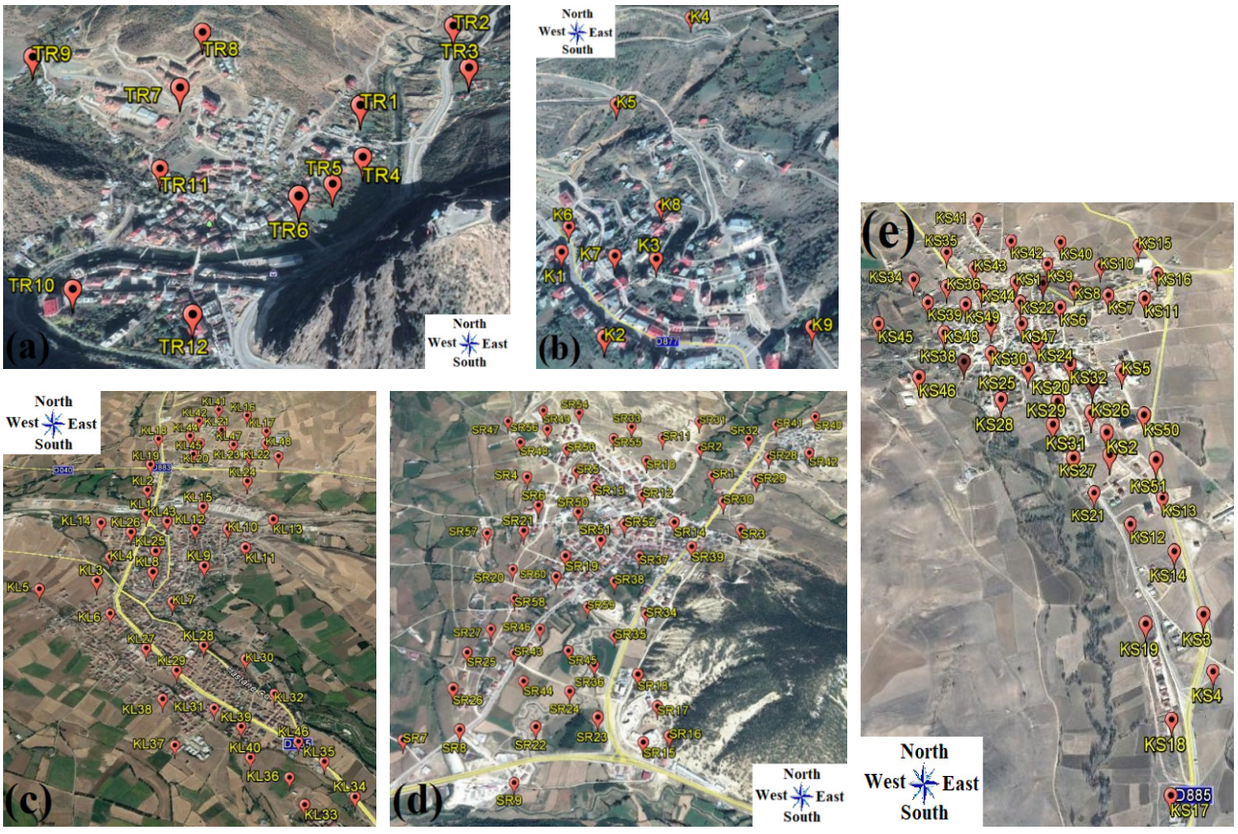

Figure 4. "Google Earth" images of the study areas and microtremor measurement points for: (a) Torul, (b) Kürtün, (c) Kelkit, (d) Şiran and (e) Köse districts.

***Kg*-value (seismic vulnerability index) Estimation from H/V Spectral Ratio**

In recent years, a lot of studies have been achieved to define the liquefaction potential (weak points) of a soil and to estimate the damage/strain of buildings and ground during a strong/large earthquake by using vulnerability index (*Kg*-value) estimated from microtremor data [9,10,13,15]. *Kg*-value can be estimated by using the amplification factor (H/V ratio) and the predominant frequency obtained from microtremor measurement as following [9,10]:

$$Kg = \frac{Ag^2}{Fg} \tag{7}$$

where *Ag* is the amplification factor and *Fg* is the predominant frequency. It is suggested that soil is susceptible to large deformation if *Kg*-value is over 20.0 and the regions in which have a value larger than 10 can be considered as the locations in risk, whereas *Kg*-values are very low in undamaged/risk-free regions [9,10]. It is possible to appraise the vulnerability of a point-based site under strong ground motion. *Kg*-value can be calculated for both soil and structures since it is related to the natural vibration period and amplification factor [9]. Thus, *Kg*-value is a parameter depending on the dynamic properties of soil and weak/strong regions can be defined by using this value for study areas and damage probability can be estimated.

RESULTS AND DISCUSSIONS

Previous studies show that two important site response characteristics (predominant frequency and amplification factor) can be estimated safely. Therefore, we used the single station microtremor data in order to identify the ground type characteristics for Torul, Kürtün, Kelkit, Şiran and Köse districts of Gümüşhane. Single station micotremor data was recorded at 12 points in Torul, 9 points in Kürtün, 48 points in Kelkit, 60 points in Şiran and 51 points in Köse. Since the site conditions were more suitable in Kelkit, Şiran and Köse, more measurements were taken in these districts. Thus, predominant frequencies and H/V ratios were obtained for each measurement points in all districts. Three components microtremor signals with resolution windows on microtremor records and the H/V spectral ratio curves with average H/V for selected points of TR7, K3, KL9, SR27

and KS38 were given as the representative examples for each region. These randomly selected examples were plotted in Figure 5. The obtained spectra include the standard deviations for all the H/V curves and the standard deviations were plotted by two dashed lines above and below of the H/V curves. All estimated values from these H/V curves as well as the other information of the points were also given in Tables 1 to 5. These selected figures show the final data processing steps (defined above) that was applied to all the microtremor measurements in the study region. These sequences of data processing implemented in the representative samples includes the interpretation of H/V curves. In these context, these primary and essential steps were involved in all the recorded microtremor data (not shown for all 180 points, only 5 measurements) in the study area. When considered the largest amplitudes of spectrum, the predominant peak in the H/V spectral rate is much more evident as a single peak with the maximum amplitude in some points (limp grounds with soft padding). However, the maximum amplitude in some points is shown in high frequencies as the multiple peaks (solid grounds). It is stated that the H/V ratios exhibit a clear peak in a soft soil structure underlying a hard rock and these peaks are constant in space and time [12]. Therefore, these peaks can be thought as predominant frequencies of the region. However, a second peak value can be observed in most of microtremor measurements. The peak with maximum amplitude can be false peak in the H/V curves with multiple peaks. In this situation, the frequencies estimated in the H/V graphics can be too small or too large to be expected according to the existing ground type. When examined all the values given in Tables, the maximum frequency estimated from horizontal amplitude spectrum on the H/V spectral rate curves is around 10 Hz and these results are accordance with the vertical amplitude spectrum values. For this reason, all the results were calculated by using the peak values (there are not multiple peaks in our data) in the H/V ratios. The H/V ratios were analyzed according to the SESAME [23] reliability criteria. It was seen that all results were generally found to provide reliable H/V curve criteria. However, unreliable H/V ratios were not included in the evaluations. Thus, the spectral amplitudes of Torul, Kürtün, Kelkit, Şiran and Köse were estimated on the maximum peaks which are compatible with the ground structure they were measured.

As mentioned above, this study aims to contribute to the classification of the ground types from microtremor data for different districts of Gümüşhane province of Turkey. The analyses of microtremor measurements in different parts of

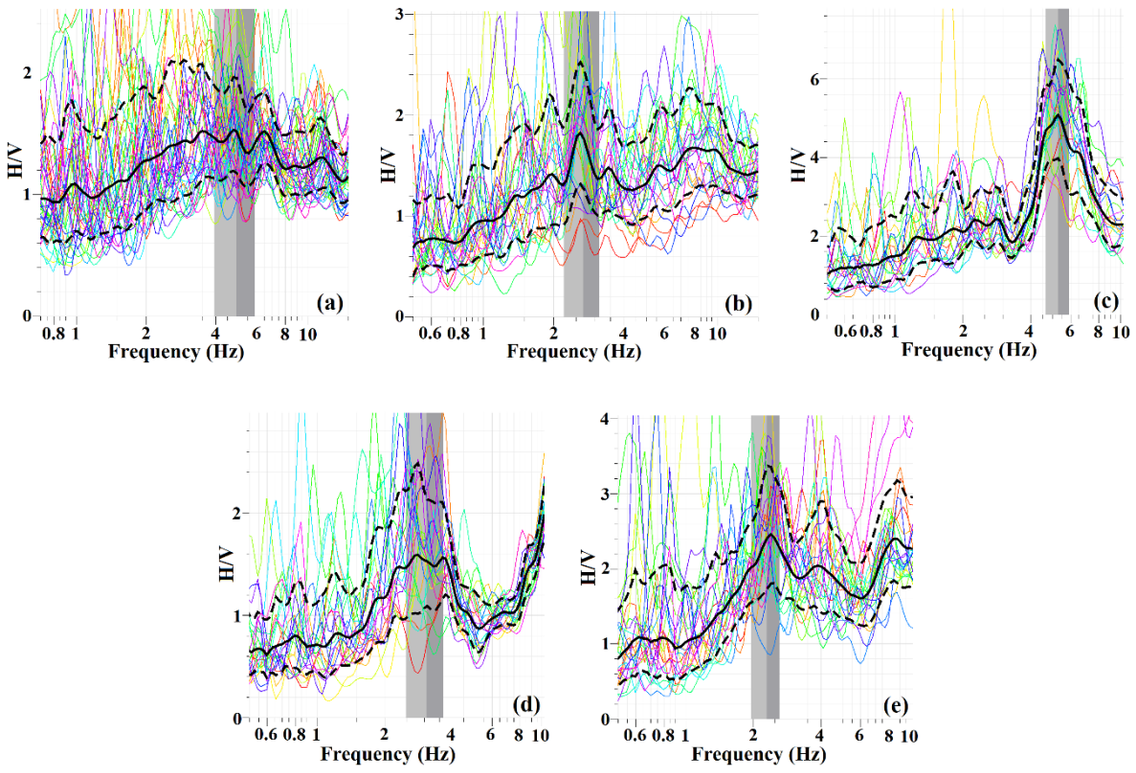

Figure 5. Examples of the H/V spectral ratio curves (solid black lines) and their standard deviations (dashed black lines) from different measurement points for: (a) TR7, (b) K3, (c) KL9, (d) SR27 and (e) KS38, respectively. Examples from each district were selected as randomly.

the world show that obtained results are useful to define the subsurface soil profiles and to build the earthquake-resistant design. The principal subject in the geotechnical researches and in detecting of the site response properties is to define the subsoil types. There are a large number of studies such as Nogoshi and Igarashi [25] and Panah et al. [26] for the ground type classifications. Nogoshi and Igarashi (1970) suggested a general classifications of ground types for Hakodate City in Hokkaido, and Panah et al. [26] proposed a classification based on the H/V spectral ratio technique in eastern and central Iran. Predominant frequencies were used in both studies as a main factor, and these works are based on the dynamic subsurface properties such as frequency, amplification, period, alluvial thickness etc. In addition to these studies, Kanai and Tanaka [11] stated that the changes in microtremor periods are related to the subsoil type. They proposed that a relatively strong peak is recorded between the periods 0.1 and 0.6s if there is a simple stratified subsurface ground. However, if subsoil properties are complicated, more than two peaks can come in sight, which one of them is small around 0.2s and the other is large around 1.0s. A sharp peak can be seen between 0.1 and 0.2s (Z_1 subsoil type) on a mountain whereas this peak can be recorded between 0.2 and 0.4s (Z_2 subsoil type) for hard diluvial formation. In some records, the curves do not have regular shapes and several peaks can appear between 0.4 and 0.8s (Z_3 subsoil type) on soft alluvial soils. In addition to these soil types, some peaks vary from 0.05 to 0.1s and from 1.0 to 2.0s (Z_4 subsoil type) especially on soft soils. Thus, Kanai and Tanaka [11] suggested that microtremor amplitudes increase at ground surface in these periods. Since Nakamura [1] technique has been widely used for the evaluation of predominant periods of the soil, we preferred this model in order to identify the ground type classifications for the study region. These classifications by Kanai and Tanaka [11] were given in detailed in Table 6.

H/V ratios give information about the stability of ground and are inversely proportional to strength of the measured area. Wave amplitude propagating in a limp ground grows in proportion to the weakness of the medium. Great H/V ratios can be obtained if the medium is weak, whereas small H/V ratios can be observed if the medium is strong [27]. However, a region with large H/V ratio cannot be said to have a limp structure and it should be supported with different techniques to confirm this result. When examining the H/V ratios given in Tables 1 to 5 and the regional variation maps plotted in Figures 6 to 10, H/V ratios are generally seen to be inversely proportional with subsoil types. In general, the largest H/V ratios were calculated for Z_2 class and the smaller values were obtained for Z_1 and Z_3 classes. Therefore, the regions including sandy gravel, stiff sandy clay, loam or sandy alluvial deposits whose depths are 5m or greater will further enlarge the ground response compared to the other environments such as stiff rock composed of gravel, sand and other soils mainly consisting of tertiary or older layers. Considering all the study regions, the H/V ratios can be said to be consistent with the ground on which they were measured (Tables 1–5). Considering the importance in microzonatin studies, it is obvious that the calculated H/V ratios and regional variation maps for different districts of Gümüşhane can provide contribution to knowledge in establishing the reliable ground-structure interaction, to settlement planning and to determine the safe areas.

As in the H/V ratios, the predominant frequency (or predominant period) values also provide information about the weakness and stability of the medium. Detailed information of total 180 single station microtremor measurements was given in Tables 1 to 5, respectively. As seen in Tables 1 to 5, predominant frequency values vary from 1.27 to 9.83 Hz and H/V ratios from 1.01 to 9.58 for all districts. Regional changes maps of these three desired parameters for all study regions were also given in Figures 6 to 10 as the "3D Google earth images". Except some measurement points in Torul, Kürtün and Şiran districts (e.g., TR3, K3, K6, K9, SR10, SR14, SR25, SR28, SR29, SR30, SR52), estimated predominant frequency values generally changes between 3.0–9.8 and the H/V peak amplitude values about between 1.0–2.0 (Tables 1, 2 and 4). This situation can be commented as a discrepancy between the near surface geology of the studied districts and the estimated soil types. However, according to the ground type classification of Kanai and Tanaka (1961), these regions mostly coincide with Z_1 subsoil type and therefore, it can be said that the amplification factor will not have an effective role in the event of a possible ground motion. In addition, K6 and K9 are the points with the highest H/V ratios of Kürtün district with their low frequency and high amplitude values. Similarly, SR28, SR29 and SR30 points of Şiran district have the largest H/V ratios of this region with their low frequency and high amplitude values. In the regions with dense settlements around the center of Kelkit, we estimated low frequency and large amplitude values whereas the frequency values are relatively large and H/V ratios are small in the areas outside the district settlement (Figures 8a, b). Since Kelkit district carries the effects of the 1992 Erzincan earthquake to a high extent, the settlement established in this district have been built as low-rise buildings. It can be said that Köse, which generally includes low frequency and large H/V ratios, has the weakest ground structure among all districts of Gümüşhane. The H/V peak amplitude values in Köse are mostly at 2.0–3.7 levels. According to results seen in Figures 6c, 7c, 8c, 9c and 10c, subsoil types of Z_1, Z_2 and Z_3 can be suggested for different districts of Gümüşhane province. Torul and Kürtün districts include the types of Z_1 and Z_2 whereas Kelkit, Şiran and Köse districts can be defined as Z_3 type as well standard grounds other than type Z_1, Z_2 or Z_4. These results show that subsurface grounds including Z_3 type subsoil, sandy gravel, sand clay and alluvial deposits were detected in Kelkit, Şiran and

Köse. These types of subsoils were observed in and around: *i*) Kelkit Aydın Doğan Vocational High School and Şehit Osman Şahin Primacy School for Kelkit district, *ii*) Köse Public Hospital, Köse İrfan Can Vocational High School and Dormitory Directorate for Köse district, *iii*) Şiran Mustafa Beyaz Vocational High School and Gözde indoor sport saloon for Şiran district.

In addition to H/V ratios, *Kg*-values were determined to assess the soil liquefaction potential of study areas. *Kg*-values were computed with Equation (7) by dividing H/V ratios to predominant frequencies and the results for all districts were given in Tables 1 to 5. Akkaya [9] were computed the vulnerability indexes of buildings and identified the effect of local soil conditions and building properties on the damage levels. In this work, the limit of *Kg*-values was given as *i*) $Kg \leq 3$ low, *ii*) $3 < Kg \leq 5$ moderate, *iii*) $5 < Kg \leq 10$ high and *iv*) $Kg \geq 10$ very high. As shown in Tables 1 to 5, *Kg*-values changes between 0.12 and 22.94 for all districts. However, locally, several high and very high *Kg*-values were observed in and around: *i*) Kürtün Yukarı-Uluköy Hanyani Mosque (point K6, *Kg*=5.81), *ii*) Kelkit district center (point KL26, *Kg*=5.16) and Şehit Osman Şahin Primary School (point KL26, *Kg*=5.46), *iii*) Şiran Atatürk Secondary School (point SR2, *Kg*=6.77) and Şiran Bus Station and its surrounding area (points SR34, SR35 and SR36, *Kg*-value between 19.75 and 22.94), *iv*) Köse National Education Directorate and its vicinity (points KS22 and KS23, *Kg*-value between 5.80 and 10.07). However, the rest *Kg*-values generally vary from 0.12 to 4.89 the other parts of Gümüşhane districts. Akkaya [9] stated that *Kg*-value can be used to define both the weak points of soil and earthquake damage before a strong/large earthquake and this parameter can supply the level of surface layer vulnerability to deformation during earthquakes. Thus, these results indicate that higher *Kg*-values in the given areas are composed of weak soil and the sites with $Kg > 5.0$ are the possible regions that structural damage can occur.

Therefore, subsoil types in these areas may be considered as weaker than the other regions due to the clay and alluvial layers they contain. Hence, it can be said that there may be some problematic grounds in these regions. Considering all districts of Gümüşhane, we observed clear differences from point-to-point and it can be interpreted that this is because the surface geology has different alteration degrees in these parts. In land measurements, we observed that ground layers have different properties from region-to-region. Although the near surface geology exhibits hard ground characteristics such as volcanic rocks or granitoid, some parts of the surface geologies were observed as muddy, gravel and loose alluvial material. Therefore, it may be wrong to make a ground classification only considering the predominant frequencies. Although the resonance peak amplitude is not an exactly reliable indicator of the amplification, significantly different values can indicate different geology and ground types. Consequently, obtained results are highly related to near surface geology and suggest that predominant frequencies, H/V ratios and *Kg*-values vary in relation to the soil formation.

It is quite important to determine the physical, mechanical or seismic parameters of the ground accurately and reliably for the identification of the ground-structure interaction. Correct and reliable engineering services for constructions in the urbanization are of great importance in the reducing the effects of blasting in which is made rock and mine quarries, and the effects of the natural events such as earthquakes. Also, these types of engineering applications can supply significant information in order to prevent or to minimize the great damages and losses caused

Table 1. Geographical coordinates, predominant frequencies, predominant periods, H/V ratios, *Kg*-values and subsoil types of 12 microtremor measurement points in Torul (TR)

Measurement Points	Longitude (Degrees)	Latitude (Degrees)	Predominant Frequency (Hz)	H/V Ratio	Predominant Period (s)	*Kg*-value	Ground Type
TR1	39.2965	40.5615	9.46	1.25	0.11	0.17	Z_1
TR2	39.3004	40.5665	8.95	2.03	0.11	0.46	Z_1
TR3	39.3001	40.5632	2.86	1.22	0.35	0.52	Z_2
TR4	39.2964	40.5595	4.57	1.06	0.22	0.25	Z_2
TR5	39.2956	40.5586	5.06	1.13	0.19	0.25	Z_1
TR6	39.2948	40.5581	6.41	2.00	0.16	0.62	Z_1
TR7	39.2915	40.5613	4.93	1.51	0.20	0.46	Z_2
TR8	39.2919	40.5630	6.81	1.51	0.15	0.33	Z_1
TR9	39.2866	40.5632	6.96	1.60	0.14	0.37	Z_1
TR10	39.2905	40.5560	9.84	1.39	0.10	0.20	Z_1
TR11	39.2914	40.5591	5.41	1.51	0.18	0.42	Z_1
TR12	39.2929	40.5553	5.92	1.40	0.17	0.33	Z_1

Table 2. Geographical coordinates, predominant frequencies, predominant periods, H/V ratios, *Kg*-values and subsoil types of 9 microtremor measurement points in Kürtün (K)

Measurement Points	Longitude (Degrees)	Latitude (Degrees)	Predominant Frequency (Hz)	H/V Ratio	Predominant Period (s)	*Kg*-value	Ground Type
K1	39.0853	40.7022	6.80	2.18	0.15	0.70	Z_1
K2	39.0864	40.7006	6.88	2.46	0.15	0.88	Z_1
K3	39.0872	40.7017	2.67	1.77	0.37	1.17	Z_2
K4	39.0877	40.7070	8.84	1.13	0.11	0.14	Z_1
K5	39.0859	40.7054	9.37	1.07	0.11	0.12	Z_1
K6	39.0853	40.7028	2.59	3.88	0.39	5.81	Z_2
K7	39.0864	40.7019	3.71	1.90	0.27	0.97	Z_2
K8	39.0872	40.7028	3.18	1.83	0.31	1.05	Z_2
K9	39.0897	40.7003	2.69	2.99	0.37	3.23	Z_2

Table 3. Geographical coordinates, predominant frequencies, predominant periods, H/V ratios, *Kg*-values and subsoil types of 48 microtremor measurement points in Kelkit (KL)

Measurement Points	Longitude (Degrees)	Latitude (Degrees)	Predominant Frequency (Hz)	H/V Ratio	Predominant Period (s)	*Kg*-value	Ground Type
KL1	39.4333	40.1352	3.90	2.01	0.26	1.04	Z_2
KL2	39.4327	40.1382	3.24	1.23	0.31	0.47	Z_2
KL3	39.4305	40.1278	9.54	2.07	0.10	0.45	Z_1
KL4	39.4311	40.1304	6.84	1.96	0.15	0.56	Z_1
KL5	39.4259	40.1270	1.75	2.82	0.57	4.54	Z_3
KL6	39.4324	40.1249	1.45	2.43	0.69	4.07	Z_3
KL7	39.4374	40.1259	3.60	1.48	0.28	0.61	Z_2
KL8	39.4352	40.1287	5.11	4.36	0.19	3.72	Z_1
KL9	39.4396	40.1293	5.28	5.08	0.19	4.89	Z_1
KL10	39.4412	40.1333	8.87	3.49	0.11	1.37	Z_1
KL11	39.4430	40.1312	8.58	3.56	0.12	1.47	Z_1
KL12	39.4381	40.1333	3.16	1.36	0.32	0.59	Z_2
KL13	39.4453	40.1344	3.17	1.37	0.32	0.59	Z_2
KL14	39.4292	40.1341	2.70	2.97	0.37	3.27	Z_2
KL15	39.4385	40.1360	3.18	2.91	0.31	2.66	Z_2
KL16	39.4417	40.1483	4.05	2.43	0.25	1.46	Z_2
KL17	39.4440	40.1460	4.41	2.49	0.23	1.41	Z_2
KL18	39.4324	40.1452	3.38	1.97	0.30	1.15	Z_2
KL19	39.4323	40.1416	4.28	2.09	0.23	1.02	Z_2
KL20	39.4370	40.1445	3.34	1.32	0.30	0.52	Z_2
KL21	39.4391	40.1463	3.36	1.34	0.30	0.53	Z_2
KL22	39.4454	40.1426	5.27	2.00	0.19	0.75	Z_1
KL23	39.4424	40.1426	4.97	3.17	0.20	2.02	Z_2
KL24	39.4425	40.1393	4.80	2.84	0.21	1.68	Z_2
KL25	39.4350	40.1309	5.16	4.56	0.19	4.03	Z_1
KL26	39.4323	40.1330	5.20	5.18	0.19	5.16	Z_1
KL27	39.4361	40.1219	3.11	1.68	0.32	0.91	Z_2
KL28	39.4405	40.1221	1.27	1.86	0.79	2.72	Z_3

(*continues*)

Table 3. Continued

Measurement Points	Longitude (Degrees)	Latitude (Degrees)	Predominant Frequency (Hz)	H/V Ratio	Predominant Period (s)	*Kg*-value	Ground Type
KL29	39.4388	40.1201	7.48	3.36	0.13	1.51	Z_1
KL30	39.4439	40.1210	7.48	3.36	0.13	1.51	Z_1
KL31	39.4420	40.1174	9.06	2.42	0.11	0.65	Z_1
KL32	39.4463	40.1184	8.98	2.40	0.11	0.64	Z_1
KL33	39.4487	40.1111	2.59	1.75	0.39	1.18	Z_2
KL34	39.4520	40.1116	4.54	1.01	0.22	0.22	Z_2
KL35	39.4500	40.1137	2.60	1.73	0.38	1.15	Z_2
KL36	39.4476	40.1127	1.40	2.52	0.72	4.54	Z_3
KL37	39.4396	40.1146	8.85	1.62	0.11	0.30	Z_1
KL38	39.4381	40.1178	4.72	1.40	0.21	0.42	Z_2
KL39	39.4440	40.1160	6.06	1.44	0.17	0.34	Z_1
KL40	39.4449	40.1140	3.13	1.01	0.32	0.33	Z_2
KL41	39.4385	40.1492	1.84	3.17	0.54	5.46	Z_3
KL42	39.4365	40.1476	3.75	2.33	0.27	1.45	Z_2
KL43	39.4354	40.1342	4.42	4.08	0.23	3.77	Z_2
KL44	39.4358	40.1456	2.75	1.75	0.36	1.11	Z_2
KL45	39.4365	40.1429	3.09	1.81	0.32	1.06	Z_2
KL46	39.4482	40.1151	2.90	1.51	0.34	0.79	Z_2
KL47	39.4406	40.1443	8.20	2.60	0.12	0.82	Z_1
KL48	39.4441	40.1444	7.62	2.46	0.13	0.79	Z_1

Table 4. Geographical coordinates, predominant frequencies, predominant periods, H/V ratios, *Kg*-values and subsoil types of 60 microtremor measurement points in Şiran (SR)

Measurement Points	Longitude (Degrees)	Latitude (Degrees)	Predominant Frequency (Hz)	H/V Ratio	Predominant Period (s)	*Kg*-value	Ground Type
SR1	**39.1302**	40.1936	5.32	4.90	0.19	4.51	Z_1
SR2	39.1299	40.1958	5.41	6.05	0.18	6.77	Z_1
SR3	39.1308	40.1895	6.93	1.86	0.14	0.50	Z_1
SR4	39.1187	40.1931	6.80	2.72	0.15	1.09	Z_1
SR5	39.1218	40.1936	6.59	2.93	0.15	1.30	Z_1
SR6	39.1194	40.1912	6.45	2.83	0.16	1.24	Z_1
SR7	39.1130	40.1793	4.71	2.21	0.21	1.04	Z_2
SR8	39.1156	40.1797	4.68	2.09	0.21	0.93	Z_2
SR9	39.1181	40.1777	4.87	2.43	0.21	1.21	Z_2
SR10	39.1262	40.1945	2.46	1.78	0.41	1.29	Z_3
SR11	39.1275	40.1964	3.14	1.87	0.32	1.11	Z_2
SR12	39.1257	40.1921	3.14	1.86	0.32	1.10	Z_2
SR13	39.1228	40.1926	3.79	1.86	0.26	0.91	Z_2
SR14	39.1273	40.1903	2.78	2.12	0.36	1.62	Z_2
SR15	39.1239	40.1791	3.10	1.62	0.32	0.85	Z_2
SR16	39.1251	40.1793	4.76	1.85	0.21	0.72	Z_2
SR17	39.1247	40.1805	4.67	1.85	0.21	0.73	Z_2
SR18	39.1240	40.1819	4.75	2.03	0.21	0.87	Z_2

(*continues*)

Table 4. Continued

Measurement Points	Longitude (Degrees)	Latitude (Degrees)	Predominant Frequency (Hz)	H/V Ratio	Predominant Period (s)	*Kg*-value	Ground Type
SR19	39.1208	40.1881	3.94	1.91	0.25	0.93	Z_2
SR20	39.1179	40.1874	3.87	1.96	0.26	0.99	Z_2
SR21	39.1185	40.1895	3.96	1.96	0.25	0.97	Z_2
SR22	39.1191	40.1798	8.00	3.09	0.12	1.19	Z_1
SR23	39.1219	40.1801	8.04	3.05	0.12	1.16	Z_1
SR24	39.1207	40.1814	8.05	3.11	0.12	1.20	Z_1
SR25	39.1157	40.1831	2.98	1.60	0.34	0.86	Z_2
SR26	39.1151	40.1814	3.17	1.45	0.32	0.66	Z_2
SR27	39.1168	40.1842	3.07	1.53	0.33	0.76	Z_2
SR28	39.1340	40.1949	2.53	2.43	0.39	2.33	Z_2
SR29	39.1327	40.1931	2.14	2.65	0.47	3.28	Z_3
SR30	39.1304	40.1917	2.40	2.38	0.42	2.36	Z_3
SR31	39.1302	40.1980	5.16	2.24	0.19	0.97	Z_1
SR32	39.1332	40.1964	5.33	2.05	0.19	0.79	Z_1
SR33	39.1256	40.1971	5.06	2.52	0.19	1.26	Z_1
SR34	39.1248	40.1850	3.89	9.24	0.26	21.95	Z_2
SR35	39.1231	40.1840	4.00	9.58	0.25	22.94	Z_2
SR36	39.1220	40.1825	3.93	8.81	0.25	19.75	Z_2
SR37	39.1250	40.1883	7.40	4.28	0.14	2.48	Z_1
SR38	39.1234	40.1868	7.20	4.35	0.14	2.63	Z_1
SR39	39.1279	40.1886	7.17	4.46	0.14	2.77	Z_1
SR40	39.1378	40.1979	8.06	2.18	0.12	0.59	Z_1
SR41	39.1352	40.1975	5.85	2.48	0.17	1.05	Z_1
SR42	39.1365	40.1950	8.34	1.97	0.12	0.47	Z_1
SR43	39.1180	40.1831	7.04	4.87	0.14	3.37	Z_1
SR44	39.1185	40.1818	7.22	4.34	0.14	2.61	Z_1
SR45	39.1207	40.1833	6.98	4.48	0.14	2.88	Z_1
SR46	39.1193	40.1843	7.13	4.40	0.14	2.72	Z_1
SR47	39.1175	40.1976	6.31	3.50	0.16	1.94	Z_1
SR48	39.1183	40.1958	6.21	4.04	0.16	2.63	Z_1
SR49	39.1198	40.1982	6.33	3.22	0.16	1.64	Z_1
SR50	39.1217	40.1908	4.64	1.65	0.22	0.59	Z_2
SR51	39.1229	40.1892	4.52	1.67	0.22	0.62	Z_2
SR52	39.1244	40.1902	2.96	1.71	0.34	0.99	Z_2
SR53	39.1212	40.1953	9.43	2.43	0.11	0.63	Z_1
SR54	39.1222	40.1980	6.68	1.41	0.15	0.30	Z_1
SR55	39.1243	40.1961	6.42	1.41	0.16	0.31	Z_1
SR56	39.1200	40.1967	6.79	1.41	0.15	0.29	Z_1
SR57	39.1164	40.1895	4.04	1.49	0.25	0.55	Z_2
SR58	39.1180	40.1858	8.21	2.27	0.12	0.63	Z_1
SR59	39.1219	40.1855	8.10	2.43	0.12	0.73	Z_1
SR60	39.1203	40.1870	8.26	2.14	0.12	0.55	Z_1

Table 5. Geographical coordinates, predominant frequencies, predominant periods, H/V ratios, *Kg*-values and subsoil types of 51 microtremor measurement points in Köse (KS)

Measurement Points	Longitude (Degrees)	Latitude (Degrees)	Predominant Frequency (Hz)	H/V Ratio	Predominant Period (s)	*Kg*-value	Ground Type
KS1	39.6524	40.2126	2.80	2.02	0.36	1.46	Z_2
KS2	39.6576	40.2047	4.33	2.39	0.23	1.32	Z_2
KS3	39.6617	40.1981	3.89	1.42	0.26	0.52	Z_2
KS4	39.6620	40.1965	3.74	1.21	0.27	0.39	Z_2
KS5	39.6581	40.2075	1.71	2.20	0.59	2.83	Z_3
KS6	39.6548	40.2109	7.96	1.46	0.13	0.27	Z_1
KS7	39.6571	40.2115	4.79	1.25	0.21	0.33	Z_2
KS8	39.6554	40.2120	7.99	1.50	0.13	0.28	Z_1
KS9	39.6538	40.2136	4.44	1.69	0.23	0.64	Z_2
KS10	39.6565	40.2134	4.44	1.41	0.23	0.45	Z_2
KS11	39.6588	40.2113	5.44	1.67	0.18	0.51	Z_1
KS12	39.6589	40.2013	2.91	1.62	0.34	0.90	Z_2
KS13	39.6601	40.2022	3.81	1.85	0.26	0.90	Z_2
KS14	39.6606	40.2002	4.14	1.61	0.24	0.63	Z_2
KS15	39.6584	40.2146	6.34	2.18	0.16	0.75	Z_1
KS16	39.6594	40.2128	6.09	2.67	0.16	1.17	Z_1
KS17	39.6607	40.1933	3.96	2.03	0.25	1.04	Z_2
KS18	39.6606	40.1952	3.47	2.16	0.29	1.34	Z_2
KS19	39.6596	40.1979	2.27	2.12	0.44	1.98	Z_3
KS20	39.6554	40.2063	4.87	1.09	0.21	0.24	Z_2
KS21	39.6573	40.2025	4.83	1.04	0.21	0.22	Z_2
KS22	39.6528	40.2114	1.36	3.70	0.73	10.07	Z_3
KS23	39.6565	40.2070	1.46	2.91	0.68	5.80	Z_3
KS24	39.6541	40.2091	6.01	2.75	0.17	1.26	Z_1
KS25	39.6538	40.2078	6.16	2.54	0.16	1.05	Z_1
KS26	39.6569	40.2056	6.09	4.72	0.16	3.66	Z_1
KS27	39.6578	40.2038	2.71	2.72	0.37	2.73	Z_2
KS28	39.6529	40.2065	2.70	2.67	0.37	2.64	Z_2
KS29	39.6553	40.2052	3.23	2.91	0.31	2.62	Z_2
KS30	39.6520	40.2088	3.52	2.73	0.28	2.12	Z_2
KS31	39.6563	40.2038	3.15	2.61	0.32	2.16	Z_2
KS32	39.6557	40.2079	5.38	2.67	0.19	1.32	Z_1
KS33	39.6568	40.2069	5.46	2.39	0.18	1.05	Z_1
KS34	39.6472	40.2130	3.32	2.55	0.30	1.96	Z_2
KS35	39.6485	40.2146	4.00	2.84	0.25	2.02	Z_2
KS36	39.6490	40.2125	4.14	2.38	0.24	1.37	Z_2
KS37	39.6508	40.2083	2.66	2.30	0.38	1.99	Z_2
KS38	39.6495	40.2099	2.29	2.39	0.44	2.50	Z_3
KS39	39.6483	40.2116	2.66	2.34	0.38	2.06	Z_2
KS40	39.6543	40.2150	4.33	2.18	0.23	1.10	Z_2
KS41	39.6497	40.2166	2.79	3.45	0.36	4.27	Z_2
KS42	39.6517	40.2151	3.07	3.14	0.33	3.21	Z_2

(*continues*)

Table 5. Continued

Measurement Points	Longitude (Degrees)	Latitude (Degrees)	Predominant Frequency (Hz)	H/V Ratio	Predominant Period (s)	*Kg*-value	Ground Type
KS43	39.6502	40.2135	7.71	2.31	0.13	0.69	Z_1
KS44	39.6508	40.2122	7.63	2.11	0.13	0.58	Z_1
KS45	39.6463	40.2103	3.89	1.15	0.26	0.34	Z_2
KS46	39.6490	40.2074	5.57	1.11	0.18	0.22	Z_1
KS47	39.6531	40.2102	3.66	2.13	0.27	1.24	Z_2
KS48	39.6516	40.2103	3.77	2.08	0.27	1.15	Z_2
KS49	39.6502	40.2114	3.83	2.21	0.26	1.28	Z_2
KS50	39.6592	40.2054	1.93	2.22	0.52	2.55	Z_3
KS51	39.6597	40.2035	2.05	1.66	0.49	1.34	Z_3

Table 6. Ground types classification of Kanai and Tanaka [11]

Type of subsoil	Subsurface ground properties
Z_1	Stiff rock composed of gravel, sand and other soils mainly consisting of tertiary or older layers
Z_2	Sandy gravel, stiff sandy clay, loam or sandy alluvial deposits whose depths are 5m or greater
Z_3	Standard grounds other than type Z_1, Z_2 or Z_4 (alluvial deposits whose depths are 5m or greater)
Z_4	Soft alluvium-delta lands and pit whose depth is 30m or greater. Reclaimed land from swamps or muddy shoal where the ground depth is 2m or greater and less than 20 years have passed since the reclamation

by explosions in the residential area on the weak ground. Therefore, the knowledge of predominant frequency of the ground and structure will allow to avoid the possible resonance and thus, the changing the frequency of ground and/or structure will make contribution to the reduction possible damages. In recent years, microtremor technique has been used to describe the local ground conditions, especially in engineering seismology studies. Also, this technique has a significant application area and is of great importance among the geophysical techniques due to its simplicity, applicable, accuracy and reliability. Thus, the availability of microtremor measurements has increased and microtremor survey method has started to be applied in order to determine different site characteristics such as spectral amplification and predominant frequency (or period) of the grounds, and to demonstrate the local ground structure interaction. Therefore, this study can be a guide and source for the future related engineering fields in different parts of Gümüşhane since it includes useful information related to the seismicity and local subsurface structure. Estimated parameters such as predominant frequency and period, H/V ratio, *Kg*-value are quite important for the microzonation studies. These parameters can also be used in the selection of earthquake recording stations. Since a microzonation study was not previously performed for Gümüşhane province which has few earthquake activity, sufficient amount of single station microtremor measurements were taken in the present study. As a remarkable fact, obtained single station microtremor recordings can also be considered as the preliminary preparation for the subsequent geophysical studies in Torul, Kürtün, Köse, Şiran, Kelkit, and it can be said that microtremor technique must be absolutely and reliably taken into account in the determining the reliable ground structure interaction since the estimations of ground classifications in all study regions were verified with actual near surface deposits.

CONCLUSIONS

In recent years, the microtremor survey method has gained popularity in seismic microzonation studies and in the estimation of ground types. The main purpose of this study is to detect the site response characteristics for Torul, Kürtün, Kelkit, Şiran and Köse districts of Gümüşhane province, Turkey. For this purpose, we used the ratio of the horizontal to vertical components of Fourier amplitude spectra, designated as H/V spectral ratio model of Nakamura technique based on the single station microtremor data analysis. In this context, predominant frequency, H/V ratio and *Kg*-value were estimated, and subsurface ground types were made according to the predominant periods for a total of 180 measurement points including all districts.

Predominant frequency changes between 2.86 and 9.84 Hz, H/V ratio between 1.06 and 2.03 for Torul district. In addition, predominant frequency varies from 2.59 to 9.37 Hz, H/V ratio from 1.07 to 3.89 for Kürtün district; predominant frequency from 1.27 to 9.54 Hz, H/V ratio from 1.01 to 5.12 for Kelkit district; predominant frequency from

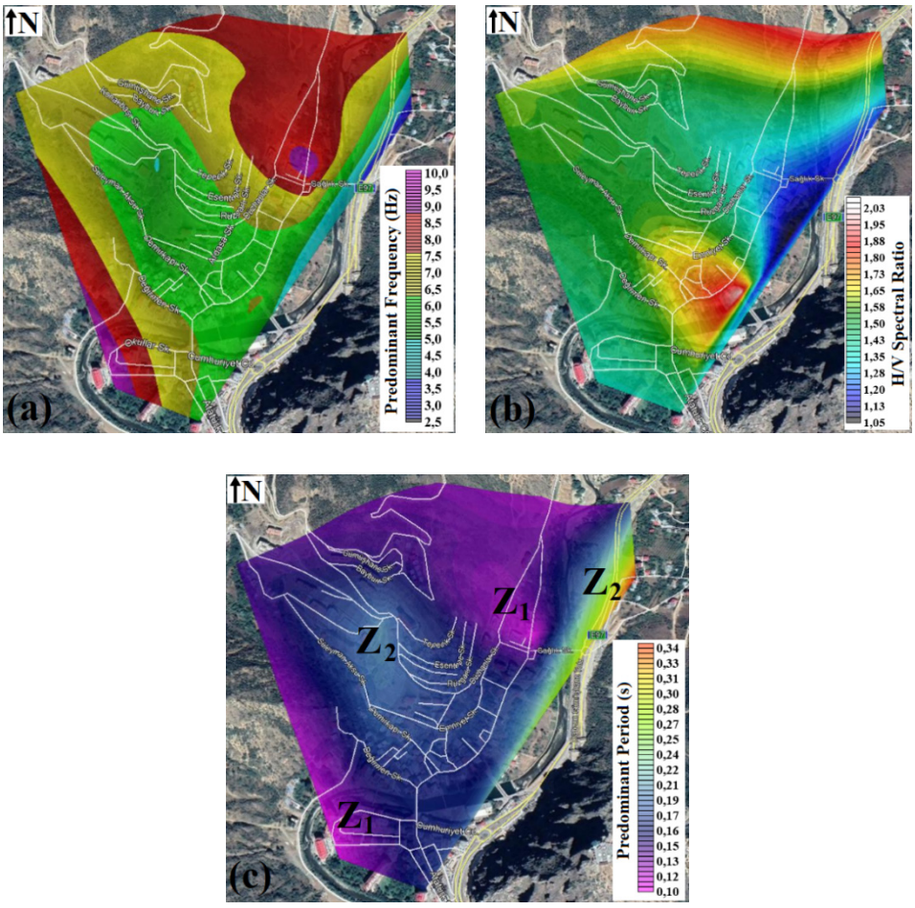

Figure 6. "Google Earth" images of Torul district for (a) Predominant frequency, (b) H/V spectral ratio and (c) Subsurface ground profiles from predominant period.

2.14 to 9.43 Hz, H/V ratio 1.41 to 9.58 for Şiran district; predominant frequency from 1.36 to 7.99 Hz, H/V ratio 1.04 to 4.72 for Köse district. According to these values, we can suggest three main ground types such Z_1 including stiff rock composed of gravel, sand and other soils mainly consisting of tertiary or older layers, Z_2 including sandy gravel, stiff sandy clay, loam or sandy alluvial deposits whose depths are 5m or greater, and Z_3 including standard grounds other than type Z_1, Z_2 or Z_4 (alluvial deposits whose depths are 5m or greater). According to these results, subsurface grounds including Z_3 type subsoil were detected in and around Kelkit Aydın Doğan Vocational High School and Şehit Osman Şahin Primacy School for Kelkit district, Köse Public Hospital, Köse İrfan Can Vocational High School and Dormitory Directorate for Köse district, Şiran Mustafa Beyaz Vocational High School and Gözde indoor sport saloon for Şiran district. Also, some high and very high *Kg*-values were detected in and around Kürtün Yukarı-Uluköy Hanyani Mosque, Kelkit district center, Kelkit Şehit Osman Şahin Primary School, Şiran Atatürk Secondary School, Şiran Bus Station and its surrounding area, Köse National Education Directorate and its vicinity. In terms of the risk assessment, these results show that the grounds in these mentioned settlements are not suitable for the next constructions. Also, obtained findings may be significant for taking necessary precautions in constructing engineering projects in these areas. These conclusions show that predominant frequencies, H/V ratios and *Kg*-values highly correspond to these subsurface ground types, and there is a good correlation among the H/V ratio, predominant frequency and actual near surface deposits. These findings can serve as the primary data sources for the other geophysical, geological and geotechnical studies such as seismic hazard microzonation and seismic site response works for Torul, Kürtün, Kelkit, Şiran and Köse districts of Gümüşhane province. As an important result, accurate and reliable surveys including the microtremor measurements could be one of the useful methods for seismic microzonation and disaster mitigation, even when detailed seismic hazard data or soil profile data is not available.

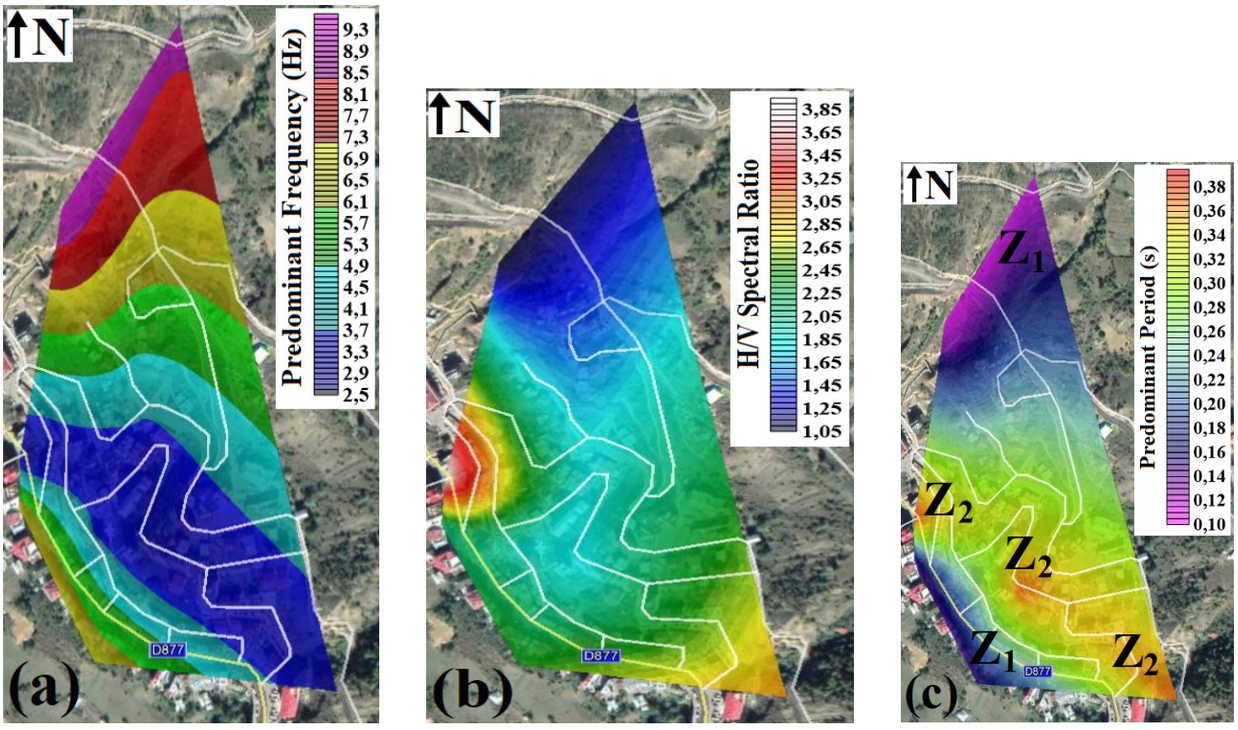

Figure 7. "Google Earth" images of Kürtün district for (a) Predominant frequency, (b) H/V spectral ratio and (c) Subsurface ground profiles from predominant period.

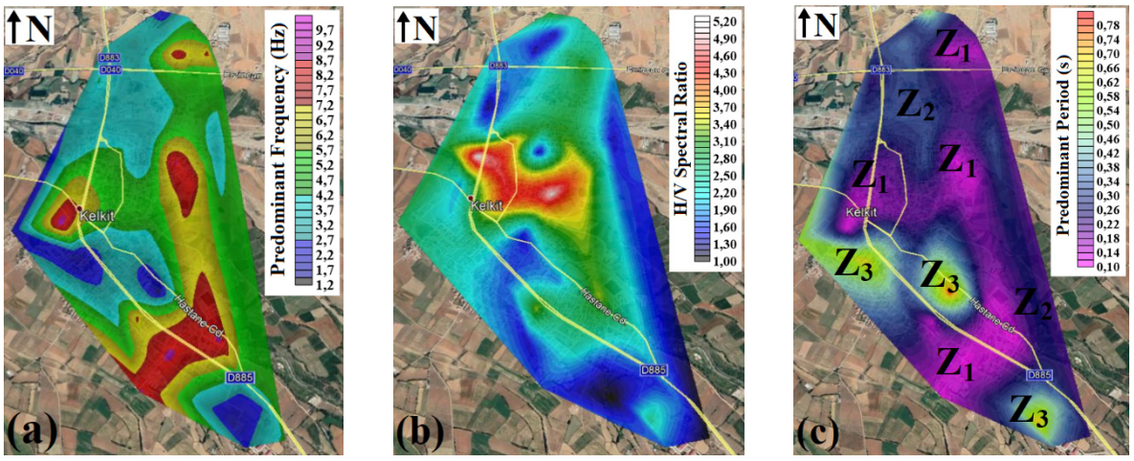

Figure 8. "Google Earth" images of Kelkit district for (a) Predominant frequency, (b) H/V spectral ratio and (c) Subsurface ground profiles from predominant period. The areas with Z_3 ground type were mentioned in the text.

ACKNOWLEDGMENT

This study is supported by Gümüşhane University Scientific Research Project (GUBAP, Turkey) with project no 17.F5117.02.01. I thank to the editor and anonyms reviewers for their useful and constructive comments, discussions and suggestions in improving this paper.

AUTHORSHIP CONTRIBUTIONS

Authors equally contributed to this work.

DATA AVAILABILITY STATEMENT

The authors confirm that the data that supports the findings of this study are available within the article. Raw

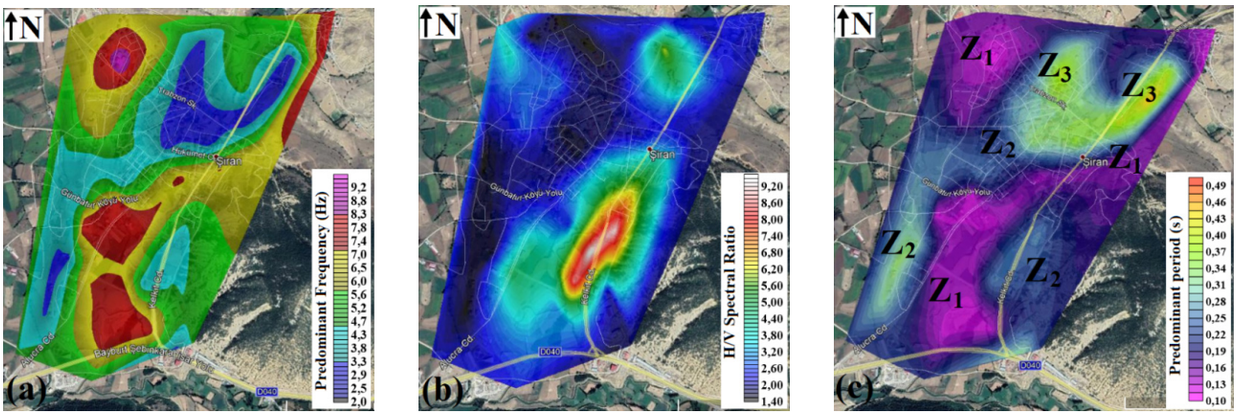

Figure 9. "Google Earth" images of Şiran district for (a) Predominant frequency, (b) H/V spectral ratio and (c) Subsurface ground profiles from predominant period. The areas with Z_3 ground type were mentioned in the text.

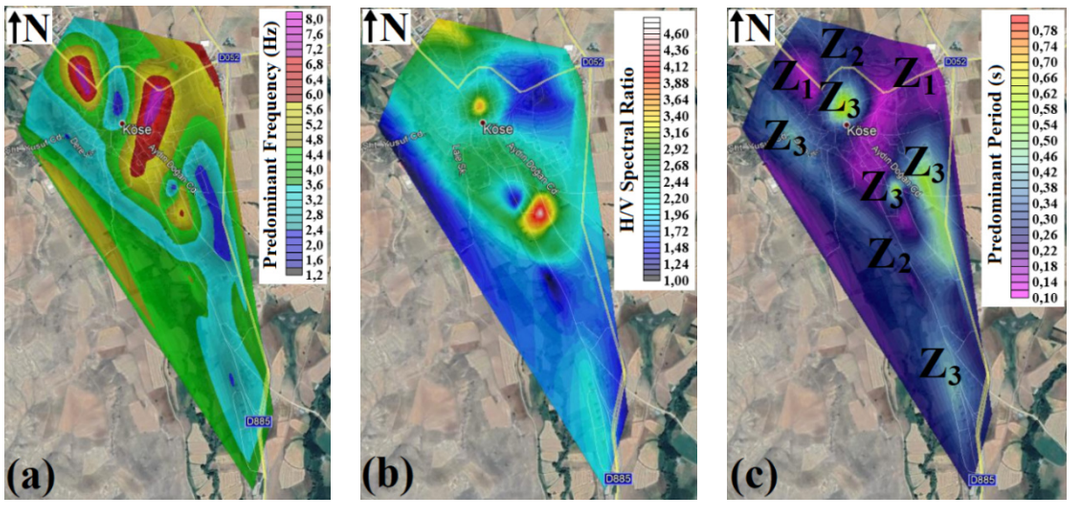

Figure 10. "Google Earth" images of Köse district for (a) Predominant frequency, (b) H/V spectral ratio and (c) Subsurface ground profiles from predominant period. The areas with Z_3 ground type were mentioned in the text.

data that support the finding of this study are available from the corresponding author, upon reasonable request.

CONFLICT OF INTEREST

The author declared no potential conflicts of interest with respect to the research, authorship, and/or publication of this article.

ETHICS

There are no ethical issues with the publication of this manuscript.

REFERENCES

[1] Nakamura Y. A method for dynamic characteristics estimation of subsurface using microtremor on the ground surface. Quarterly Report of Railway Technical Res Inst 1989;30:25–33.

[2] Haile M, Seo K, Kurita K, Kyuke H, Yamanaka H, Yamazaki K, et al. Study of site effects in Kobe area using microtremors. Journal of Physics of the Earth 1997;45:121–33. [CrossRef]

[3] Gosar A, Martinec M. Microtremor HVSR study of site effects in the Ilirska Bistrica town area (S. Slovenia). Journal of Earthquake Engineering 2009;13:50–67. [CrossRef]

[4] Vella A, Galea P, D'Amico S. Site frequency response characterization of the Maltese islands based on ambient noise H/V ratios, engineering geology. 2013;163:89–100. [CrossRef]

[5] Rincon O, Shakoor A, Ocampo M. Investigating the reliability of H/V spectral ratio and image entropy for quantifying the degree of disintegration of weak rocks, engineering geology. 2016;207:115–28. [CrossRef]

[6] Singh AP, Parmar A, Chopra S. Microtremor study for evaluating the site response characteristics in the Surat city of western India. Natural Hazards 2017;89:1145–66. [CrossRef]

[7] Babacan AE, Akın Ö. The investigation of soil-structure resonance of historical buildings using seismic refraction and ambient vibrations HVSR measurements: a case study from Trabzon in Turkey. Acta Geophysica 2018;66:1413–33. [CrossRef]

[8] Fat-Helbary RES, El-Faragawy KO, Hamed A. Application of HVSR technique in the site effects estimation at the south of Marsa Alam city, Egypt. Journal of African Earth Sciences 2019;154:89–100. [CrossRef]

[9] Akkaya İ. Availability of seismic vulnerability index (K_g) in the assessment of building damage in Van, Eastern Turkey, Earthquake Engineering and Engineering Vibration. 2020;19:189–204. [CrossRef]

[10] Babacan AE, Ceylan S. Evaluation of soil liquefaction potential with a holistic approach: a case study from Araklı (Trabzon, Turkey), Bollettino di Geofisica Teorica ed Applicata. 2021;62:173–98.

[11] Kanai K, Tanaka T. On microtremors. Bulletin of the Earthquake Research Institute 1961;39:97–114.

[12] Adib A, Afzal P, Heydarzadeh K. Site effect classification based on microtremor data analysis using a concentration–area fractal model. Nonlinear Processes in Geophysics 2015;22:53–63.

[13] Rezaei S, Choobbasti AJ. Application of the microtremor measurements to a site effect study. Earthquake Science 2017;30:157–64. [CrossRef]

[14] Mukhopadhyay S, Bormann P. Low cost seismic microzonation using microtremor data: an example from Delhi, India. Journal of Asian Earth Sciences 2004:24:271–80. [CrossRef]

[15] Beroya AAA, Aydin A, Tiglao R, Lasala M. Use of microtremor in liquefaction hazard mapping. Engineering Geology 2009;107:140–53. [CrossRef]

[16] Sanchez-Sesma FJ, Rodriguez M, Iturraran-Viveros U, Luzon F, Campillo M, Margerin L, Garcia-Jerez A, Suarez M, Santoyo MA, Rodriguez-Castellanos A. A theory for microtremor H/V spectral ratio: application for a layered medium. Geophysical Journal International 2011;186:221–5. [CrossRef]

[17] Pandey AK, Roy PNS, Baidya PR, Gupta AK. Estimation of current seismic hazard using Nakamura technique for the Northeast India. Natural Hazards 2018;93:1013–27.

[18] Taş N, Okumuş E, Öner Ş, Köksal C, İcat MY, Tanış S, ve ark. Gümüşhane il çevre durum raporu. Gümüşhane Valiliği İl Çevre ve Orman Müdürlüğü, Gümüşhane, Türkiye. 2003;179.

[19] Şaroğlu F, Emre Ö, Kuşcu İ. Active fault map of Turkey, General Directorate of Mineral Research and Exploration, Ankara, Turkey, 1992.

[20] Bozkurt E. Neotectonics of Turkey-a synthesis. Geodinamica Acta 2001;14:3–30. [CrossRef]

[21] Öztürk S. Regional and temporal variations of current earthquake activity in and around Gümüşhane: A statistical assessment (in Turkish with English abstract). Gümüşhane University Journal of Science and Technology Institute 2017;7:25–40.

[22] Nakamura Y. On the H/V spectrum, The 14th World Conference on Earthquake Engineering (WCEE), October 12–17, Beijing, China, 2018.

[23] SESAME. Guidelines for the implementation of the H/V spectral ratio technique on ambient vibrations measurements, processing and interpretation, SESAME European Research Project, WP12-Deliverable D23.12, Europan Commission Research General Directorate. 2004; Project No. EVG1-CT-2000-00026:62.

[24] Konno K, Ohmachi T. Ground-motion characteristics estimated from spectral ratio between horizontal and vertical components of microtremor. Bulletin of the Seismological Society of America 1998;88:228–41. [CrossRef]

[25] Nogoshi M, Igarashi T. On the propagation characteristics of microtremors. Journal of the Seismological Society of Japan 1970;23:264–80. [CrossRef]

[26] Panah AK, Moghaddas NH, Ghayamghamian MR, Motosaka M, Jafari MK, Uromieh A. Site effect classification in East-Central of Iran. Journal of Seismology and Earthquake Engineering 2002;4:37–46.

[27] Beker Y. Determination of soil properties by microtremor method in KTU campus, Master thesis, Karadeniz Technical University, Trabzon, Turkey. 2011:127.

[28] URL-1. Available from: http://www.mta.gov.tr/mta_web/haritalar.asp. Accessed on December 26, 2007.